

**Prediction of the Maximum Compressive Strength Geopolymers Using the Method of  
Weighted Chemical Compositions of Binders**

Tatsuya Koumoto, Ph.D.<sup>1\*</sup>

Hyung-Been Kang, Ph.D.<sup>2</sup>

Ai Takahashi, M.Sc.<sup>3</sup>

Shinya Komoto, Ph.D.<sup>4</sup>

<sup>1</sup> Professor Emeritus of Saga University, Saga 840-8502, Japan  
koumotot@cc.saga-u.ac.jp

\* Corresponding author

<sup>2</sup> XRD Specialist, Engineering Section, Okinawa Institute of Science and Technology  
Graduate University (OIST), 1919-1 Tancha, Onna-son, Okinawa, 904-0495, Japan  
hyungbeen.kang@oist.jp

<sup>3</sup> Research Support Technician, Imaging Section, Okinawa Institute of Science and  
Technology Graduate University (OIST), 1919-1 Tancha, Onna-son, Okinawa, 904-0495,  
Japan  
ai.takahashi@oist.jp

<sup>4</sup> Imaging Specialist, Imaging Section, Okinawa Institute of Science and Technology Graduate  
University (OIST), 1919-1 Tancha, Onna-son, Okinawa, 904-0495, Japan  
shinya.komoto@oist.jp

26

27   **Abstract:** Geopolymers are composite hard materials made by mixing solid binders such as  
28   fly ash and slag and alkaline liquid activators such as NaOH and sodium silicate.  
29   Geopolymers have recently been developed to be used as a replacement for Portland cement  
30   concrete. Industrial by-products such as fly ash, steel making slags and garbage melting  
31   furnace slags can be used to create geopolymers in a process that emits less carbon dioxide  
32   than in the cement making process. This reduction in CO<sub>2</sub> emission is important because CO<sub>2</sub>  
33   is one of the substances known to contribute to global warming. In the future, further uses of  
34   these fly ash and slags must be explored. The development of high compressive strength  
35   geopolymers using fly ash and slags will strongly contribute to the fields of construction,  
36   geotechnical engineering, and architecture. The compressive strength of geopolymers,  $q_u$ , is  
37   generally considered to be a function of the weight ratio of activator to binder,  $w$ , and the  
38   weight ratio of NaOH to sodium silicate,  $\eta$ . The maximum compressive strength,  $q_{umax}$  were  
39   determined as the maximum value among the peak values of  $q_u$  which were obtained for  
40   various values of  $w$  and  $\eta$ . The values of  $w$  and  $\eta$  which yield the maximum compressive  
41   strength,  $q_{umax}$  are defined as the optimum values  $w_{opt}$  and  $\eta_{opt}$  respectively. When designing  
42   the geopolymer works, it is essential to establish the method to predict the  $q_{umax}$  using the  
43   chemical compositions of binders only. This research is firstly to clarify the chemical and  
44   physical properties of geopolymer materials by using SEM and XRD observation, and

secondly the mechanical properties of the  $q_{umax}$ , and lastly to find out the method to predict the  $q_{umax}$  by combining three chemical compositions of  $\text{SiO}_2$ ,  $\text{Al}_2\text{O}_3$  and  $\text{CaO}$  in binders.

## Introduction

More than 60 billion kgs of industrial by-products such as fly ash, steelmaking slags, and garbage melting furnace slags are generated every year in Japan (Koumoto, 2019). Fly ash and slags can be used to create geopolymers in a process that emits less carbon dioxide than in the cement making process. This reduction in  $\text{CO}_2$  emission is important because  $\text{CO}_2$  is one of the substances known to contribute to global warming. In the future, further uses of these fly ash and slags must be explored.

The chemical mechanism for hardening composite materials by mixing aluminosilicate binders, such as fly ash, and slags with alkaline activators, such as liquid  $\text{NaOH}$  and sodium silicate, is known as a geopolymer reaction. The hardened composite material is called geopolymer (Davidovits, 1979). Geopolymers are produced by mixing two components of solid binders like fly ash, slags, etc. and liquid activators like  $\text{NaOH}$ ,  $\text{KOH}$ , sodium silicate and so on (Buchwald, 2006). Geopolymers have recently been developed to be used as a replacement for Portland cement concrete. The development of high compressive strength geopolymer using

fly ash and slags will strongly contribute to the fields of construction, geotechnical engineering, and architecture.

Koumoto, 2019 has proposed the method to produce the high compressive strength geopolymers for the above-mentioned binders with an alkaline liquid mixture composed of NaOH and sodium silicate. He has clarified that the  $w_{opt}$  which is the optimum value of  $w$  (= weight ratio of liquid and binder) yielding the maximum compressive strength  $q_{umax}$  becomes a constant value of  $w_{opt} = 0.40$  regardless of kinds of materials (see Fig. 1) and the  $\eta_{opt}$  which is the optimum value of  $\eta$  (= weight ratio of liquid NaOH and sodium silicate) yielding  $q_{umax}$  is expressed as a function of  $C_{as}(= Al_2O_3 + SiO_2)$ .

This paper describes firstly the chemical compositions, the morphological states, the crystallographic structures and the physical properties for 8 starting geopolymer materials. The mechanical characteristics of the high compressive strength geopolymers were studied to establish the method to predict the  $q_{umax}$  using the weighted chemical compositions of  $SiO_2$ ,  $Al_2O_3$  and  $CaO$  in binders. To correlate between  $q_{umax}$  and these three chemical compositions, the following weighted chemical composition method was introduced simply as:  $q_{umax} = f(\chi) = A \exp(B \times \chi)$ , where  $A$  and  $B$  are constants and  $\chi = SiO_2^\alpha \times Al_2O_3^\beta \times CaO^\gamma$  in which  $\alpha$  and  $\beta$  are smaller than 1.0, while  $\gamma$  is set as 1. The values of  $\alpha$  and  $\beta$  that gives the highest correlation ratio were determined using trial and error.

## **Materials**

### ***Preparation of Geopolymer Materials***

The finer the particle size, the greater the compressive strength of geopolymers (Koumoto, 2019). In the present tests, all slags which were provided in granular were ground after being air dried to a maximum particle size of 0.106 mm for effective chemical reaction.

### ***Chemical compositions of Geopolymer materials***

The chemical compositions of the geopolymer materials tested are obtained by the fluorometric analysis and listed in Table 1. The eight kinds of geopolymer materials (three Fly ash, two each of Slag1 (steel factory slags) and Slag2 (garbage melting furnace slags), and one Acidproof cement were the starting geopolymer materials, and the twenty three mixture materials which consist of the mixture of one Acidproof cement and Slag1, three Fly ash and Fly ash, eight Fly ash and Slag1, two Fly ash and Slag2, five Slag1 and Slag1 and four Slag1+Slag2) were prepared as geopolymer materials with a wide range of chemical compositions. In Table 1, geopolymer samples which are marked with \* are data cited from Koumoto, 2019.

## ***Physical properties of starting geopolymer materials***

The physical properties such as density of particle  $\rho_s$ , loss of ignition and brain value for 8 starting geopolymer materials are listed in Table 2.

## ***SEM observation***

Preparation of 8 starting geopolymer materials for scanning electron microscopy observation were as follow. Materials were loaded onto carbon tape and sealed on the cylinder stub (Cat. No. 1255B-100, EM Japan Co., Ltd.). 5 nm-thickness of platinum coating was carried out (Dual Head Sputter Coater Cressington 208DS, Cressington Scientific Instruments Ltd.) before being transferred to the SEM. Images were obtained by scanning electron microscope (JSM-7900F, JEOL) at accelerating voltages of 5 kV.

Fig. 2 shows SEM pictures of 8 starting geopolymer materials (2000x magnification) listed in Table 1. Typical cenospheres were observed in the Fly ash Matsuura and Reihoku, however, not in the Fly ash Karita which showed similar morphology to other slag materials (even though chemical compositions ( $\text{SiO}_2/\text{Al}_2\text{O}_3$ ) of Karita showed similar ratio to those in Fly ash Matsuura and Reihoku). Notable composition difference on Karita contain 500% more CaO and contain only half to 1/3 of  $\text{Fe}_2\text{O}_3$  to those in Matsuura and Reihoku. Karita is the pressurized fluidized

bed coal ash (PFBC ash) and accordingly Karita contains large amount of Ca component comparing to other Fly ash such as Matsuura and Reihoku (JIS ash). Fly ash Karita and other slag materials exhibit different morphology depending on their origin. Fig. 3 shows SEM pictures of Fly ash Matsuura and Reihoku (Top: x2000 & Bottom: x5000). Not only cenosphere but also pleroshpere (sphere in sphere) were clearly observed in Matsuura and Reihoku, but not in Karita. Addition to this, cenosphere found in Matsuura were not only smooth surface, but also rough and often perforated compared with Reihoku indicates that Matsuura is a mixture of magnetic cenosphere and plerosphore.

### ***XRD observation***

Fig.4 shows XRD pattern of different fly ash and slag samples. Fly ash Matsuura, Reihoku and Karita exhibit definite crystalline pattern. However, slag such as Koro, Kazusa, Narashino and Selament exhibit non-crystalline patterns which is typical of quenched slag samples and are therefore comparatively reactive in nature. Compared to this, the slag Stainless exhibits crystalline patterned and is considered comparatively less reactive (Das *et al*, 2020). Amorphous region can be observed in Fly ash Matsuura and Reihoku clearly. On the other hand, slag materials all showed very complex pattern with several overlapping peaks presumably resulting from mixture of many different minerals in the samples as previously reported

(Yildirim and Prezzi, 2011).

Fig. 5 shows the relationship between density of particle  $\rho_s$  for starting geopolymer materials (in Table 2) and each chemical composition: (a)  $\text{SiO}_2$ , (b)  $\text{Al}_2\text{O}_3$  and (c)  $\text{CaO}$  (in Table 1). In Fig. 5  $\rho_s$  largely decrease with an increase in  $\text{SiO}_2$  and  $\text{Al}_2\text{O}_3$  as well. As in Fig. 3 there are seen a lot of pleroshpere which is created from  $\text{SiO}_2$  being origin of glass,  $\rho_s$  of Fly ash Matsuura and Reihoku become smaller. On the other hand  $\rho_s$  proportionally increases with an increase in  $\text{CaO}$ , accordingly, it might be said that the amount of  $\text{CaO}$  decides the densities of geopolymer materials.

### ***Making Geopolymer Samples***

According to Koumoto, 2019, the 48%  $\text{NaOH}$  (18mol/L) and sodium silicate ( $\text{Na}_2\text{O} \cdot n\text{SiO}_2$ ,  $n=3.2$ ) were used as activators in this research. Geopolymer samples were made for  $\eta$  ranging from 0.0 to 1.0 at a constant value of  $w = w_{opt} = 0.40$ . After mixing the activator and binder, the geopolymer samples were compacted in plastic molds of diameter  $D = 50$  mm and height  $H = 100$  mm. The geopolymer samples were removed from the molds after 1 or 2 days and cured at room temperature under dry condition for 28 days.



## 149    **Test and Results**

### 150    ***Compression tests***

151    Before compression tests, diameter  $d$ , height  $h$  and weight  $W$  of all geopolymer samples were  
152    measured.

153    Compression tests of geopolymer samples were carried out at Saga Construction  
154    Technology Support Organization (SCTSO) using the concrete testing apparatus in the same  
155    test method used for concrete samples.

156    The volume shrinkage ratio  $\Delta V/V$  ( $= (V - V')/V$ ) in which  $V = \frac{1}{4}\pi D^2 H$  and  $V' = \frac{1}{4}\pi d^2 h$  are  
157    volume of plastic mold and geopolymer sample at  $q_{umax}$ , respectively and the density of  
158    geopolymer sample at  $q_{umax}$  ( $\rho_t (= W/V')$ ) were calculated.

159

### 160    **Compression test results**

161    Compression test results are shown in Fig. 6A for Fly ash, Acidproof cement, Fly ash+Fly  
162    and Fly ash+Slag1 and Fig. 6B for Fly ash+Slag1, Slag1+Slag1 and Slag1+Slag2.

163    As shown in Fig. 6A and Fig. 6B,  $q_u$  generally increase as  $\eta$  increase, and reach the maximum  
164    value  $q_{umax}$  at a certain  $\eta$  value, which is defined as the optimum value  $\eta_{opt}$ . The  $q_{umax}$  is defined

as the peak value among  $q_u$  values obtained for several  $\eta$  values. The values of  $\eta_{opt}$  and  $q_{umax}$  from Fig. 6A and Fig. 6B are summarized in Table 3. Table 3 also includes the value of  $w_{opt}$  and both values of the density of geopolymer sample at  $q_{umax}$ .

## Discussions

### *Correlation between $\eta_{opt}$ and $C_{as}(=Al_2O_3+SiO_2)$*

Because geopolymerization is a chemical reaction specially an aluminosilicate reaction, the amount of NaOH which contributes to ionize metals contained in the binder increases with the increase of the amount of  $Al_2O_3$  and  $SiO_2$ . Accordingly,  $\eta$ , which is the weight ratio of NaOH to sodium silicate, is considered as the function of  $C_{as}$  ( $=Al_2O_3+SiO_2$ ) (Koumoto, 2019).

Fig. 7 shows the correlation between  $\eta_{opt}$  from Table 3 and chemical compositions of binders  $C_{as}$  ( $=Al_2O_3+SiO_2$ ) calculated from Table 1. In Fig. 7 the relationship between  $\eta_{opt}$  and  $C_{as}$  is well correlated by the straight line with a high correlation coefficient of  $r = 0.949$  as

$$\eta_{opt} = 0.0160C_{as} - 0.453 \quad (r = 0.949) \quad (1a)$$

Equation (1a) is almost same to the equation (1b) which was proposed by Koumoto, 2019 as

$$\eta_{opt} = 0.0157C_{as} - 0.414 \quad (r = 0.949) \quad (1b)$$

From Fig. 7, the newly added fifteen compression test data points also support the equation (1b). The equation (1b) is newly proposed to calculate the  $\eta_{opt}$  value from the value of  $C_{as}$  of binders to very effectively produce high compressive strength geopolymers.

#### ***Chemical characteristic of $q_{umax}$***

Fig. 8 shows the relationship between the  $q_{umax}$  and each chemical composition  $SiO_2$ ,  $Al_2O_3$  and CaO for 8 starting geopolymer materials. In the Fig. 2, plerosphere (sphere in sphere) were found in the Matsuura and Reihoku fly ash but not in Karita, in which support the lightweight of the materials (Fig. 3 & Table 3). This supports the fact that incorporation of high volumes of cenosphere reduces the density of composites but also reduce the mechanical properties of hardened composites (Xu et al, 2015). This was indeed the case that Matsuura and Reihoku fly ash showed significantly lower compression strength ( $q_{umax}$ ) compared with Karita fly ash.

In Fig. 8 the  $q_{umax}$  decreases with increase of both  $SiO_2$  and  $Al_2O_3$ , however increases with increase of CaO except the case of Slag Stainless. The case of Stainless might be by the reason which is judged from XRD observation being less reactive. According to ZHAO et al, 2010, in the case of Fly ash Matsuura the addition of CaO proportionally increased the  $q_{umax}$  to some content of CaO of 8-10 % in weight after that  $q_{umax}$  decreased with increase of CaO. It can be

said that an increase of CaO contents in the geopolymer material contributes the increase of  $q_{umax}$  to some content.

As a result, it may be effective to correlate the factor  $C_{cas}$  ( $= CaO/C_{as}$ ;  $C_{as}=SiO_2+Al_2O_3$ ) with the mechanical properties of the high compressive strength geopolymers as Koumoto, 2019 has pointed out. Fig. 9 shows the relationship between the  $q_{umax}$  and  $C_{cas}$ . The  $q_{umax}$  increases with an increase in  $C_{cas}$  until  $C_{cas}$  reaches about 0.8 and after that the  $q_{umax}$  decreases with an increase in  $C_{cas}$ . There seems to have the  $q_{umax}$  being greater than about 150 N/mm<sup>2</sup> in the range of  $C_{cas}$  in between 0.6 and 0.9.

#### ***Volume shrinkage of geopolymer samples***

Fig. 10 shows the relationship between the volume shrinkage ratio of geopolymer sample,  $\Delta V/V$  at  $q_{umax}$  and  $C_{cas}$ . The values of  $\Delta V/V$  were generally less than 2% when  $C_{cas}$  is less than 0.95 and increased sharply with increase in the factor  $C_{cas}$ . These results will be helpful for the design of geopolymer construction work.

#### ***Prediction of $q_{umax}$ using the method of weighted chemical compositions of binders***

When designing the geopolymer works, it is essential to predict the  $q_{umax}$  using the chemical compositions of binders only. Das, et al, 2000 has proposed to clarify the behavior of the  $q_{umax}$  of industrial by-products based geopolymer samples as dependent on Al/Si, Ca/Si and Ca/(Si+Al) ratios. In the research the values of SiO<sub>2</sub>, Al<sub>2</sub>O<sub>3</sub> and CaO are directly used to develop the  $q_{umax}$  equation.

Now although Fig. 9 shows the chemical characteristics of  $q_{umax}$ , there is no linear relationship to predict the value of  $q_{umax}$ . This section is to consider to combine the weighted three chemical compositions of SiO<sub>2</sub> <sup>$\alpha$</sup> , Al<sub>2</sub>O<sub>3</sub> <sup>$\beta$</sup>  and CaO <sup>$\gamma$</sup> , where  $\alpha$ ,  $\beta$  and  $\gamma$  are powers and  $\gamma$  is set to be 1.0 as in binders and to correlate  $q_{umax}$  and  $\chi = SiO_2^\alpha \times Al_2O_3^\beta \times CaO^{1.0}$  as the equation to decide the values of  $\alpha$  and  $\beta$  by trial and error as:

$$q_{umax} = f(\chi) = Aexp(B \times \chi) \quad (2)$$

$$\text{where } \chi = SiO_2^\alpha \times Al_2O_3^\beta \times CaO^{1.0} \quad (3)$$

Fig. 11 shows the relationship between  $q_{umax}$  and  $\chi$  in the case of  $\alpha = \beta = \gamma = 1.0$ . In the Fig. 11, the relationship between  $q_{umax}$  and  $\chi$  is assumed to express as:

$$q_{umax} = Aexp(B \times \chi) \quad (4)$$

231 According to the least square method, the equation (4) is expressed with a rather high  
232 correlation coefficient as:

$$233 \quad q_{umax} = 17.74 \exp (9.48 \times 10^{-5} \times \chi) \quad (r = 0.848) \quad (5)$$

234 where  $\chi = SiO_2 \times Al_2O_3 \times CaO$ .

235

236 Now the values of  $\alpha$  and  $\beta$  were determined by trial and error to yield the highest correlation  
237 factor  $r$  to the  $q_{umax}$  equation. The obtained values of  $\alpha$  and  $\beta$  were 0.59 and 0.69,  
238 respectively.

239 Fig. 12 shows the relationship between  $q_{umax}$  and  $\chi (= SiO_2^{0.59} \times Al_2O_3^{0.69} \times CaO^{1.0})$ .

240 The  $q_{umax}$  equation according to least square method is expressed as:

$$241 \quad q_{umax} = 15.71 \exp (1.06 \times 10^{-3} \times \chi) \quad (r = 0.940) \quad (6)$$

242 where  $\chi = SiO_2^{0.59} \times Al_2O_3^{0.69} \times CaO^{1.0}$ .

243 In Fig. 12, Eq.6 is drawn by the solid line together with break lines of error for  $\pm 25\%$ .

244 Almost all the values of  $q_{umax}$  are plotted along the equation (6) in between the break lines of  
245 error for  $\pm 25\%$ ..

From the design of geopolymer construction works point of view, the following equation (7) is recommended to estimate the values of  $q_{umax}$  for designing on safe side as:

$$q_{umax} = 11.71 \exp (1.06 \times 10^{-3} \times \chi) \quad (7)$$

where  $\chi = SiO_2^{0.59} \times Al_2O_3^{0.69} \times CaO^{1.0}$ .

## Conclusions

This paper describes the chemical and mechanical characteristics of geopolymers by mixing fly ash and slags as binders with 48% NaOH (18 mol/L) and sodium silicate ( $Na_2 \cdot nSiO_2, n=3.2$ ) as activators in which geopolymer samples were made for values of  $\eta$  from 0.0 to 1.0 at a constant value of  $w = 0.40$ .

The research results are summarized as:

(a) There is an optimum value,  $\eta_{opt}$  (the weight ratio of NaOH to sodium silicate) yielding  $q_{umax}$  for each binder,

(b) The  $\eta_{opt}$  is well correlated with the factor  $C_{as}$  ( $=Al_2O_3 + SiO_2$ ) as:

$\eta_{opt} = 0.0160C_{as} - 0.453$ . The value  $\eta_{opt}$  for an arbitrary binder necessary to manufacture the high compressive strength geopolymer is calculated by the above equation.

(c) The  $q_{umax}$  increases with an increase in  $C_{cas}$  until  $C_{cas}$  value of about 0.8 and after that  $q_{umax}$  decreases with an increase in  $C_{cas}$ . There seems to have the  $q_{umax}$  being greater than about 150 N/mm<sup>2</sup> in the range of  $C_{cas}$  in between 0.6 and 0.9.

(d) The density of the fly ash sample displayed the Matsuura and Reihoku showed significantly lower (~23%) than that of Karita. In the SEM analysis, plerospheres were found in the Matsuura and Reihoku fly ash but not in Karita, in which support the lightweight of the materials (Fig. 3 & Table 2). This supports the fact that incorporation of high volumes of cenosphere reduces the density of composites but also reduce the mechanical properties of hardened composites (Xu *et al*, 2015). This was indeed the case that Matsuura and Reihoku fly ash showed significantly lower compression strength ( $q_{umax}$ ) compared with Karita fly ash.

(e)  $q_{umax}$  for Matsuura exhibited significantly low compared to not only other Fly ash samples but also to all the geopolymer materials. One interesting point is the chemical compositions of Matasuura that contain lower content of FeO and CaO which are similar percentile to those found in other Fly ash. This is contradicted to previously reported that magnetic cenosphere generally contain higher amounts of FeO, CaO (Sokol *et al*, 2000) indicating the influence of additional factors from this coal burning power plant.

(f) The volume shrinkage ratio  $\Delta V/V$  is generally less than 2% when  $C_{cas}$  is smaller than 0.95.



(g) The  $q_{umax}$  equation is expressed with high correlation index  $r = 0.940$  by using weighted

chemical compositions of  $\chi = SiO_2^{0.59} \times Al_2O_3^{0.69} \times CaO^{1.0}$  as:

$$q_{umax} = 15.71 \exp(1.06 \times 10^{-3} \times \chi) \quad \text{where } \chi = SiO_2^{0.59} \times Al_2O_3^{0.69} \times CaO^{1.0}.$$

(h) For designing of geopolymer construction works the following equation is recommended to

estimate the values of  $q_{umax}$  on safe side as:

$$q_{umax} = 11.71 \exp(1.06 \times 10^{-3} \times \chi) \quad \text{where } \chi = SiO_2^{0.59} \times Al_2O_3^{0.69} \times CaO^{1.0}.$$

## Acknowledgements

The authors are grateful to Maruwa Giken for preparing ground solid waste incinerator slags.

The authors are also grateful to Kyuden Sangyo, Shunan Works, Nissin Steel, and Nippon Steel

& Sumikin Slag Products for contributing coal-fired power plant ash, stainless manufactured

slag, and ground granulated blast slag, respectively.

## Data Availability

All data, models, and code generated or used during the study appear in the submitted article.

296

297   **References**

- 298   Biwan Xu, Hongyan Ma, Chuanlin Hu and Zongjin Li, 2015 “Influence of cenospheres on  
299   properties of magnesium oxychloride cement-based composites” Materials and Structures,  
300   DOI 10.1617/s11527-015-0578-6.
- 301   Buchwald, A., 2006 “What are geopolymers? Current state of research and technology, the  
302   opportunities they offer, and their significance for precast industry.” Betonwerk und Fertigteil  
303   Technik 72(7): 42-49.
- 304   Das, P., Koumoto, T. and Komoto, S., 2020 “Mathematical Modeling of Geopolymer  
305   Reactions”, Chapter I and Chapter II, LAMBERT Academic Publishing.
- 306   Davidovitz, J., 1991 “Geopolymers, inorganic polymeric new materials” J. Therm. Anal. 37(8):  
307   1633-1656 <https://doi.org/10.1007/BF0.1912193>.
- 308   Kojima, K. and Nakao, K., 1995 “Ground Technology Basics and Practice”, KAJIMA  
309   INSTITUTE PUBLISHING CO., LTD, p.39.

310 Kondo, F., LEGRANS, R.R.I. and Koumoto, T., 2014 “Comparison of Strength Characteristics  
 311 for Hardened Geopolymer Paste Using PFBC Fly Ash and JIS Fly Ash”, IDRE Journal, 294,  
 312 101-107.

313 Koumoto, T., 2019 “Production of High Compressive Strength Geopolymers Considering Fly  
 314 Ash or Slag Chemical Composition”, J. Mater. Civ. Eng., ASCE, 31(8) 06019006-1-  
 315 06019006-6 (2019).

316 Sokol E.V., Maksimova N.V., Volkova N.I., Nigmatulina E.N., and Frenkel A.E., 2000  
 317 “Hollow silicate microspheres from fly ashes of the Chelyabinsk brown coals (South Urals,  
 318 Russia)”, Fuel Processing Technology 67 2000 35–52.

319 Takami K., Oka Y., Katayama K. and WANG, L., 2016 “Research on the effective use of  
 320 stainless slag as a material for high-fluidity conc rete” Proc. of the Japan Concrete Institute,  
 321 vol. 38(1), 1431-1436.

322 Yildirim, I.Z. and Prezzi, M., 2011 “Chemical, Mineralogical, and Morphological Properties of  
 323 Steel Slag” Advances in Civil Engineering, doi:10.1155/2011/463638.

324 ZHAO, Y., Koumoto, T. and Kondo, F., 2010 “Effect of CaO Content in Fly Ash on the  
 325 Compressive Strength of Geopolymer”, IDRE Journal, 270, 1-7.

326

327 **Table 1. Chemical composition of tested geopolymer materials**

Geopolymer material	Geopolymer sample	Chemical composition (%)						Mixture ratio of geopolymer samples:
		SiO <sub>2</sub>	Al <sub>2</sub> O <sub>3</sub>	CaO	Fe <sub>2</sub> O <sub>3</sub>	MgO	SO <sub>3</sub>	
Fly ash	Matsuura	63.3	22.8	3.8	3.7	0.8	0.5	
	Reihoku *	55.0	21.1	9.1	5.3	1.1	0.9	
	Karita *	38.8	24.3	19.5	1.5	0.5	6.6	
Slag1	Koro *	34.6	14.8	42.7	0.4	5.7	0.0	
	Stainless *	26.7	5.3	48.2	1.0	5.5	0.4	
Slag2	Kazusa *	34.2	13.2	42.0	2.6	1.9	0.7	
	Narashino *	34.2	13.9	39.3	3.7	1.8	0.6	
Acidproof cement	Selament	49.8	13.6	26.7	2.6	--	--	
A.cement and Slag1	SelaKoro	42.2	14.2	34.7	1.5	--	--	SelaKoro: Selament:Koro=1:1 by weight
Fly ash and Fly ash	KariRei *	46.9	22.7	14.3	3.5	0.8	3.8	
	KariRei2 *	49.6	22.2	12.6	4.1	0.9	2.8	
	MatRei	59.2	22.0	6.5	4.5	1.0	0.7	MatRei: Matsuura:Reihoku=1:1 by weight
Fly ash and Slag1	ReiKoro *	44.8	18.0	25.9	2.9	3.4	0.5	
	KoroRei5	51.6	20.1	14.7	4.5	1.9	0.8	KoroRei5: Koro:Reihoku=1:5 by weight;
	ReiKoro2 *	41.4	16.9	31.5	2.0	4.2	0.3	
	ReiKoro5	38.2	15.9	37.1	1.2	4.9	0.2	ReiKoro5: Reihoku:Koro=1:5 by weight
	KariKoro *	36.7	19.5	31.1	1.0	3.1	3.3	
	KoroKari5	38.1	22.7	23.4	1.4	5.5		KoroKari5: Koro:Karita=1:5 by weight
	KariKoro2 *	36.0	18.0	35.0	0.8	4.0	2.1	
	KariKoro5	35.3	16.4	38.8	0.6	4.8	1.1	KariKoro5: Karita:Koro=1:5 by weight
	KariKoro7	35.1	16.0	39.8	0.6	5.1	0.8	KariKoro7: Karita:Koro=1:7 by weight
Fly ash and Slag2	ReiKazu *	44.6	17.2	25.6	4.0	1.5	0.8	
	ReiNara *	44.6	17.5	25.6	4.5	1.4	0.8	
Slag1 and Slag1	StaKoro5	33.3	13.2	43.6	0.5	5.7	0.1	StaKoro5: Stainless:Koro=1:5 by weight
	StaKoro2	32.0	11.6	44.5	0.8	5.6	0.1	StaKoro2: Stainless:Koro=1:2 by weight
	StaKoro	30.7	10.1	45.4	0.7	5.6	0.1	StaKoro: Stainless:Koro=1:1 by weight
	KoroSta2	29.3	8.5	46.3	0.8	5.5	0.3	KoroSta2: Stainless:Koro=1:2 by weight
	KoroSta5	28.0	6.9	47.3	0.9	5.5	0.1	KoroSta5: Koro:Stainless=1:5 by weight
Slag1 and Slag2	KazuKoro5	34.5	14.5	42.6	0.8	5.1	0.1	KazuKoro5: Kazusa:Koro=1:5 by weight
	KazuKoro2 *	34.5	14.3	42.5	1.1	4.4	0.2	
	KazuKoro *	34.4	14.0	42.4	1.5	3.8	0.4	
	KoroKazu3	34.3	13.6	42.2	2.1	2.9	0.5	KoroKazu3: Koro:Kazusa=1:3 by weight
Note: *= Data from Koumoto (2019).								

328

329

330

331

332

333

334

335

**Table 2 Physical properties of starting geopolymer materials**

Geopolymer materials	Fly ash			Slag1		Slag2		Acid-proof cement
Geopolymer sample	Matsuura	Reihoku	Karita	Koro	Stainless	Kazusa	Narashino	Selament
Density of particle(g/cm <sup>3</sup> )	2.22	2.40	2.66	2.91	3.05	2.84	2.88	2.82
Loss of Ignition (%)	2.6	1.3	6.6	0.09	5.0	0.28	0.23	1.39
Brain value (cm <sup>2</sup> /g)	4130	4020	5160	4180	5868	N/A	N/A	N/A
Specific surface (m <sup>2</sup> /g)	N/A	N/A	N/A	N/A	N/A	1.55	0.83	3.33
Note: Data for Karita are from Kondo <i>et al</i> , 2014, Data for Stainless are from Takami <i>et al</i> , 2016.								
Brain value and Specific surface were obtained by Brain method and BET method, respectively.								

348 **Table 3 Compression test results of geopolymer samples**

Geopolymer material	Geopolymer sample	Compression test results				
		$q_{\text{umax}}(\text{N/mm}^2)$	$w_{\text{opt}}$	$\eta_{\text{opt}}$	$\rho_t (\text{kg/m}^3)$	$\Delta V/V (\%)$
Fly ash	Matsuura	15.1	0.40	1.00	1522	0.40
	Reihoku*	45.2	0.40	0.80	1868	0.20
	Karita*	104.3	0.40	0.50	1985	0.20
Slag1	Koro*	168.0	0.40	0.40	2227	1.20
	Stainless*	48.1	0.40	0.00	2269	11.34
Slag2	Kazusa*	110.0	0.40	0.30	2202	1.49
	Narashino*	86.4	0.40	0.50	2043	0.80
Acidproof cement	Selament	108.0	0.40	0.45	2160	1.10
A.cement and Slag1	SelaKoro	137.0	0.40	0.44	2218	1.49
Fly ash and Fly ash	KariRei*	70.1	0.40	0.65	1971	0.80
	KariRei2*	40.9	0.40	0.70	1986	1.00
	MatRei	38.5	0.40	0.87	1780	1.40
Fly ash and Slag1	ReiKoro*	79.3	0.40	0.60	2098	0.70
	KoroRei5	54.6	0.40	0.70	2174	2.00
	ReiKoro2*	118.0	0.40	0.60	2144	1.20
	ReiKoro5	130.0	0.40	0.50	2129	2.28
	KariKoro*	117.0	0.40	0.45	2122	0.90
	KoroKari5	83.4	0.40	0.40	2113	0.99
	KariKoro2*	159.0	0.40	0.43	2149	0.70
	KariKoro5	177.0	0.40	0.39	2183	1.09
Fly ash and Slag2	ReiKazu*	102.0	0.40	0.55	2081	1.39
	ReiNara*	94.3	0.40	0.65	2024	1.89
Slag1 and Slag1	StaKoro5	135.0	0.40	0.30	2208	0.80
	StaKoro	126.0	0.40	0.25	2243	3.26
	StaKoro2	136.0	0.40	0.10	2261	2.68
	KoroSta2	86.6	0.40	0.15	2296	6.17
	KoroSta5	45.8	0.40	0.20	2349	5.69
Slag1 and Slag2	KazuKoro*	132.0	0.40	0.35	2219	1.29
	KazuKoro2*	166.0	0.40	0.36	2218	1.49
	KazuKoro5	155.0	0.40	0.36	2249	1.49
	KoroKazu3	153.0	0.40	0.40	2180	2.08
Note: * Data from Koumoto, 2019; $q_{\text{umax}}$ =maximum value of compressive strength $q_u$ ; $w_{\text{opt}}$ =optimum value of $w$ yielding $q_{\text{umax}}$ ; $\eta_{\text{opt}}$ =optimum value of $\eta$ yielding $q_{\text{umax}}$ ; $\rho_t$ =density of geopolymer sample at $q_{\text{umax}}$ ; and $\Delta V/V$ =volume shrinkage ratio of geopolymer sample.						

349

350

351

352

353

354

355 **Appendix Notation**

356 *The following symbols are used in this paper:*

357  $A$  = constant,

358  $B$  = constant,

359  $C_{as}$  =  $Al_2O_3 + SiO_2$  (%),

360  $C_{cas} = CaO/C_{as}$ ,

361  $D$  = diameter of mold (mm),

362  $d$  = diameter of geopolymer sample (mm),

363  $H$  = height of mold (mm),

364  $h$  = height of geopolymer sample (mm),

365  $q_u$  = compressive strength (N/mm<sup>2</sup>),

366  $q_{umax}$  = maximum compressive strength (N/mm<sup>2</sup>),

367  $r$  = correlation coefficient,

368  $V$  = volume of mold  $\pi D^2 H/4$  (mm<sup>3</sup>),

369  $V'$  = volume of geopolymer sample  $\pi d^2 h/4$  (mm<sup>3</sup>),

370  $w$  = weight ratio of solution of sodium hydroxide and sodium silicate to binder,

371  $w_{opt}$  = optimum value of  $w$  at yielding  $q_{umax}$ ,

372  $\Delta V$  = amount of volume shrinkage of geopolymer sample  $V-V'$  (mm<sup>3</sup>),

373  $\Delta V/V$  = volume shrinkage ratio of geopolymer sample (%),

374  $\alpha$  = power,

375  $\beta$  = power,

376  $\gamma$  = power (=1),

377  $\rho_s$  = density of particle (g/cm<sup>3</sup>),

378  $\eta$  = weight ratio of sodium hydroxide to sodium silicate,

379  $\eta_{opt}$  = optimum value of  $\eta$  at yielding  $q_{umax}$

380  $\rho_t$  = density of geopolymer sample at  $q_{umax}$  (kg/m<sup>3</sup>)

381  $\varphi$  = diameter of plate of loading

382  $\chi = SiO_2^\alpha \times Al_2O_3^\beta \times CaO^{1.0}$

383

384



385 **List of Figure Captions**

386 Fig. 1 Relationship between  $q_u$  and  $w$  for various value of  $\eta$  in each starting geopolymer  
387 materials: (a) Fly ash, (b) Slag 1 and (c) Slag 2

388 Fig. 2 SEM observation of 8 starting geopolymer materials (Mag x2000)

389 Fig. 3 Observation of Matsuura & Reihoku (Top: x2000 & Bottom: x5000)

390 Fig. 4 XRD observation of 8 starting geopolymer materials SEM results

391 Fig. 5 Relationship between density of particle  $\rho_s$  for starting geopolymer materials and each  
392 chemical composition of binders: (a)  $\text{SiO}_2$ , (b)  $\text{Al}_2\text{O}_3$  and (c)  $\text{CaO}$

393 Fig. 6A Compression test results for geopolymer samples (Fly ash, Acidproof cement, Fly ash+  
394 Fly ash and Fly ash+Fly ash)

395 Fig. 6B Compression test results for mixed binder geopolymer samples ( Fly ash+ Slag1,  
396 Slag1+Slag1 and Slag1+Slag2)

397 Fig. 7 Correlation between  $\eta_{opt}$  and  $C_{as}$

398 Fig. 8 Relationship between  $q_{umax}$  and each chemical composition: (a)  $\text{SiO}_2$ , (b)  $\text{Al}_2\text{O}_3$  and (c)  
399  $\text{CaO}$

400 Fig. 9 Relationship between  $q_{umax}$  and  $C_{cas}$

401 Fig. 10 Relationship between  $\Delta V/V$  and  $C_{cas}$

402 Fig. 11 Relationship between  $q_{umax}$  and  $\chi (= SiO_2 \times Al_2O_3 \times CaO)$

403 Fig. 12 Relationship between  $q_{umax}$  and  $\chi (= SiO_2^{0.59} \times Al_2O_3^{0.69} \times CaO^{1.0})$

404

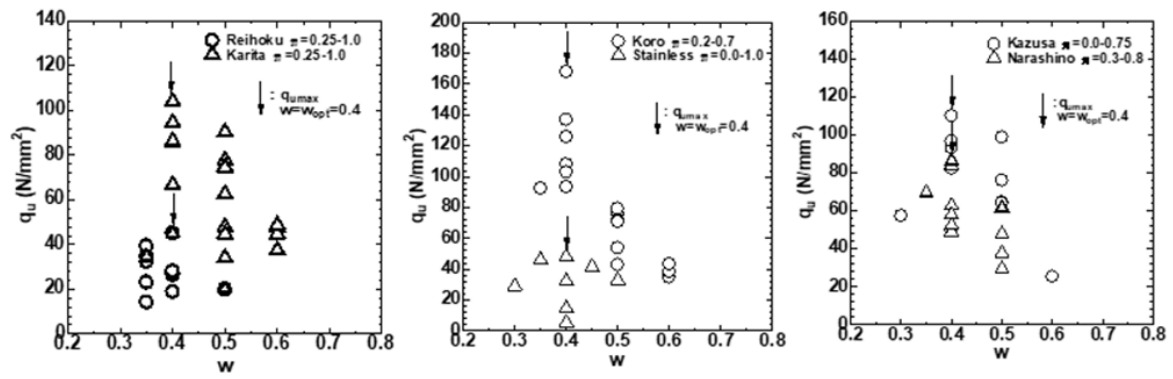


**Fig. 1 Relationship between  $q_u$  and  $w$  for various value of  $\eta$  in each starting geopolymer materials: (a) Fly ash, (b) Slag 1 and (c) Slag 2**

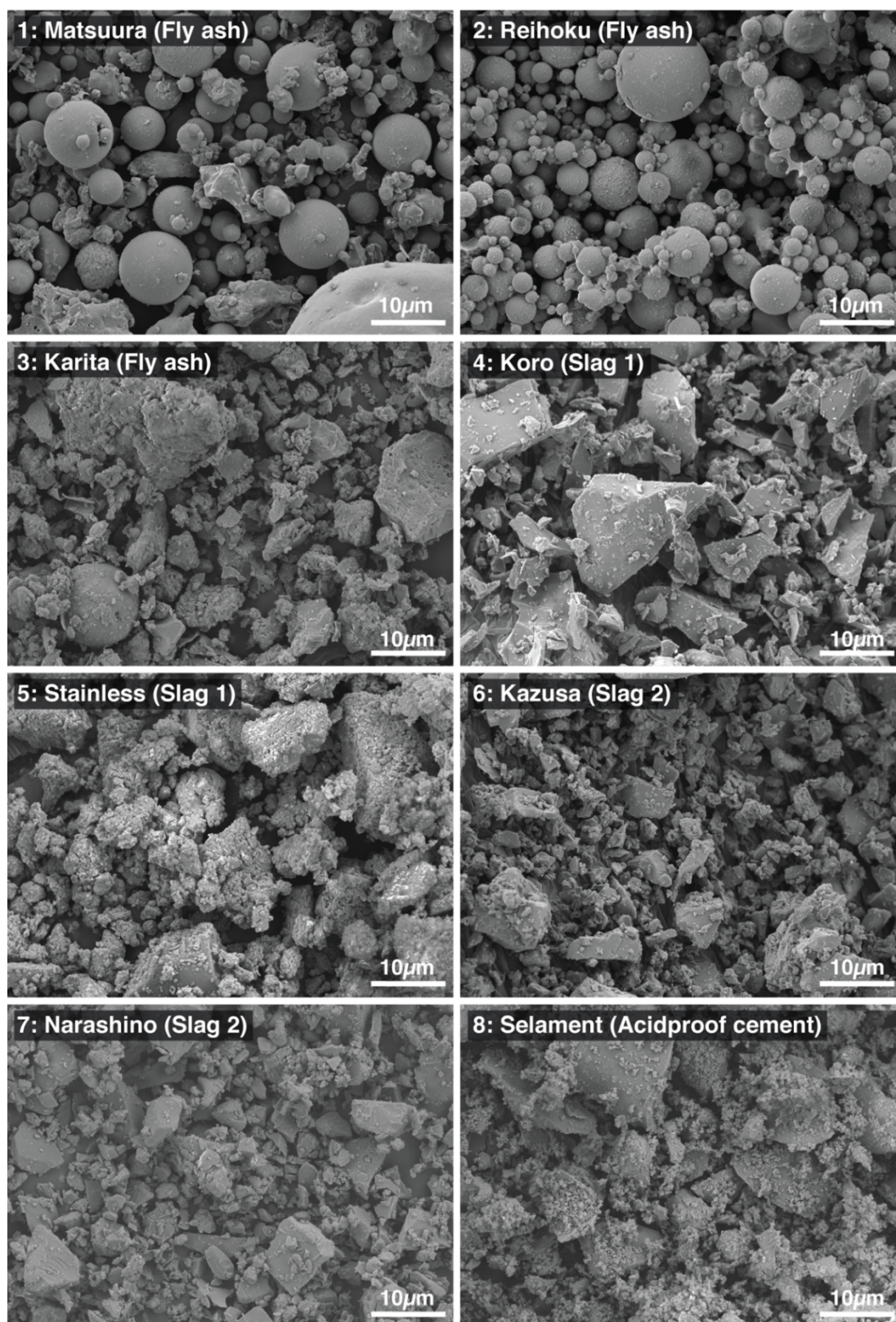


**Fig. 2 SEM observation of 8 starting geopolymer materials (Mag x2000)**



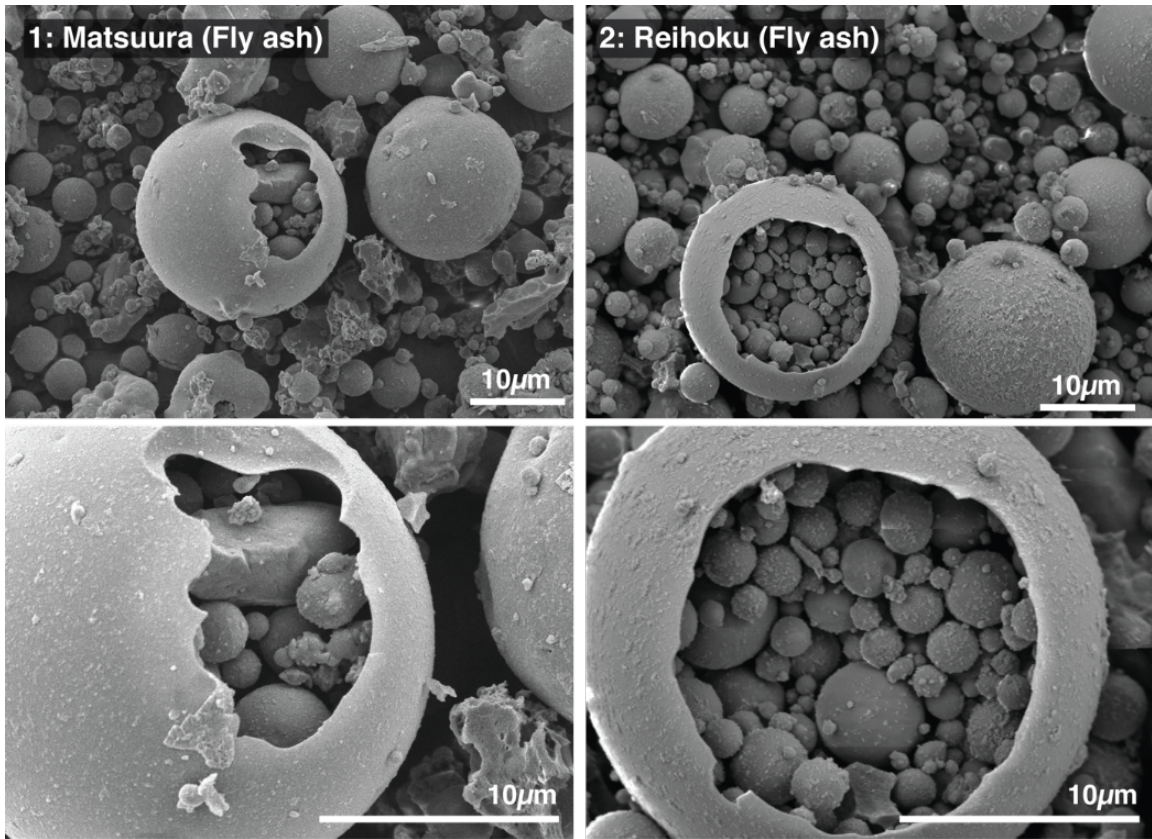
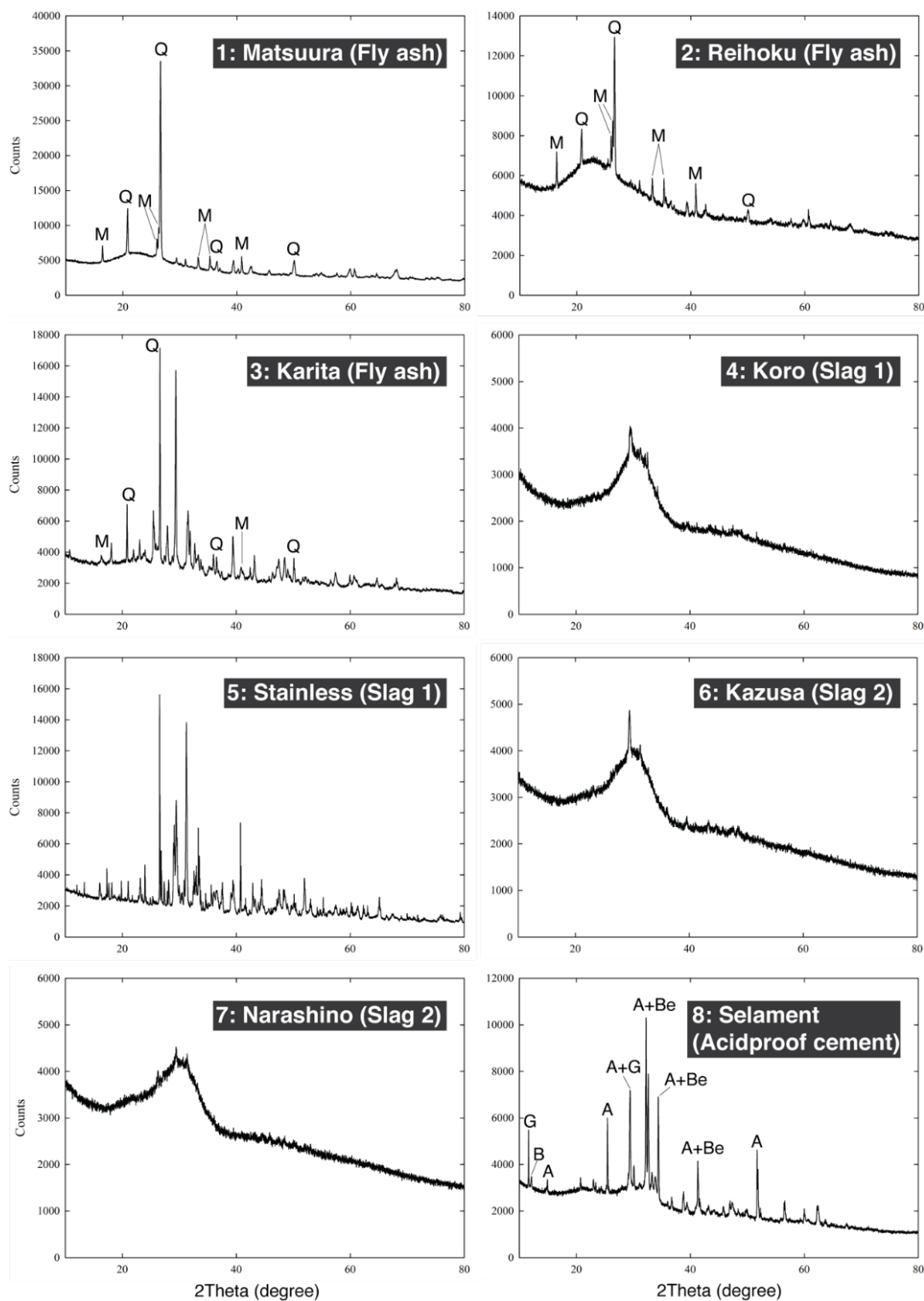


**Fig. 3 SEM observation of Matsuura & Reihoku (Top: x2000 & Bottom: x5000)**



425

426 (M=Mullite ( $\text{Al}_6\text{O}_{13}\text{Si}_2$ ); Q=Quartz ( $\text{SiO}_2$ ); G=Gypsum ( $\text{CaSO}_4 \cdot 2\text{H}_2\text{O}$ ); B=Brownmillerite ( $\text{Ca}_2(\text{Al,Fe})_2\text{O}_5$ );427 A=Alite ( $3\text{CaO} \cdot \text{SiO}_2$ ); Be=Belite ( $2\text{CaO} \cdot \text{SiO}_2$ ))

**Fig. 4 XRD observation of 8 starting geopolymer materials SEM results**

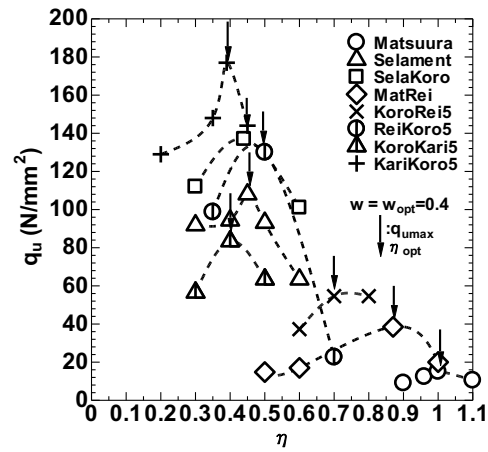


**Fig. 6A Compression test results for geopolymer samples (Fly ash, Acidproof cement, Fly ash+Fly and Fly ash+Slag1)**

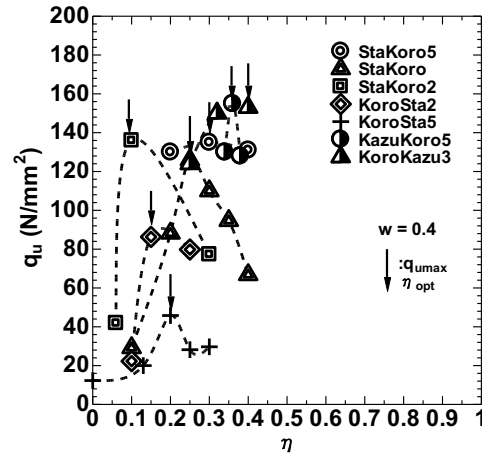


**Fig. 6B Compression test results for mixed binder geopolymer samples (Fly ash+Slag1, Slag1+Slag1 and Slag1+Slag2)**

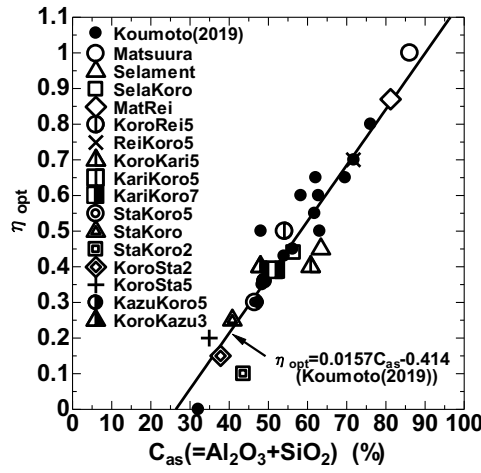


**Fig. 7 Correlation between  $\eta_{opt}$  and  $C_{as}$**



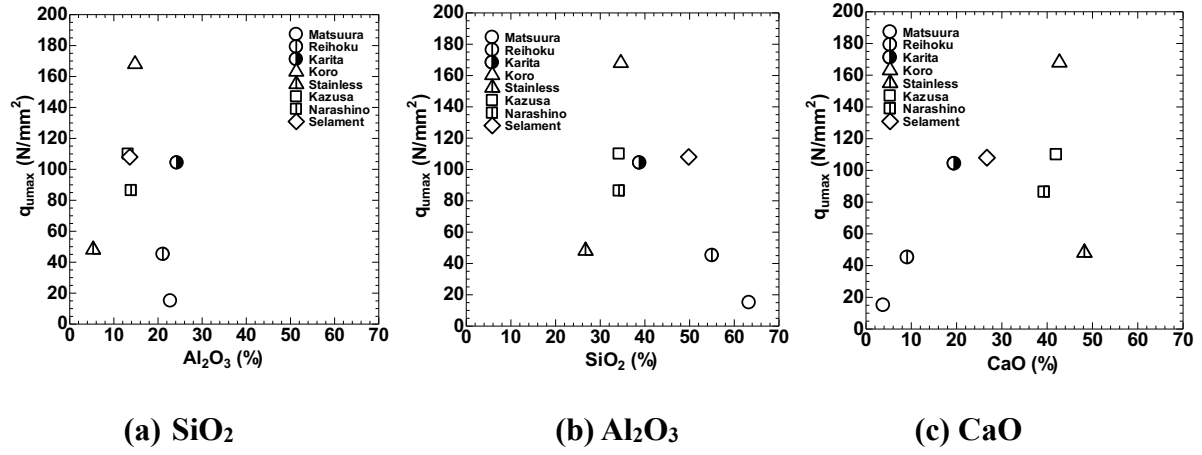


**Fig. 8 Relationship between  $q_{max}$  and each chemical composition: (a)  $SiO_2$ , (b)  $Al_2O_3$  and (c)  $CaO$  for 8 starting geopolymer materials**

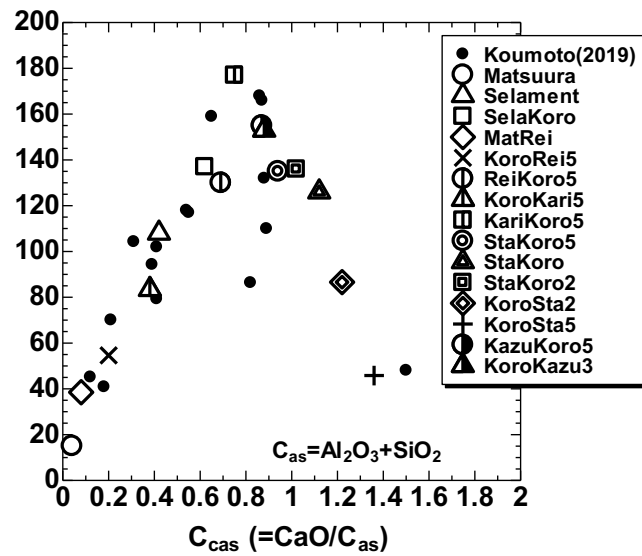


**Fig. 9 Relationship between  $q_{max}$  and  $C_{cas}$**

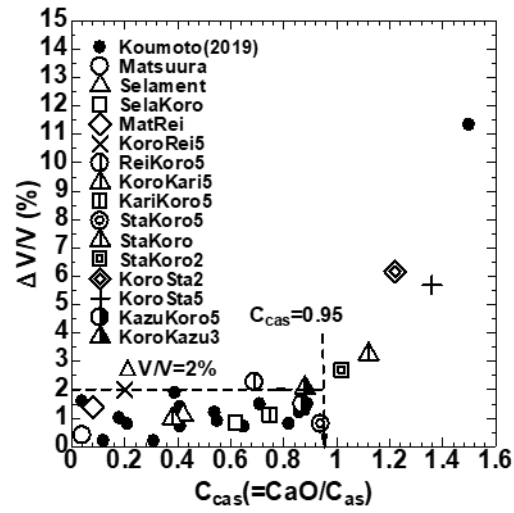
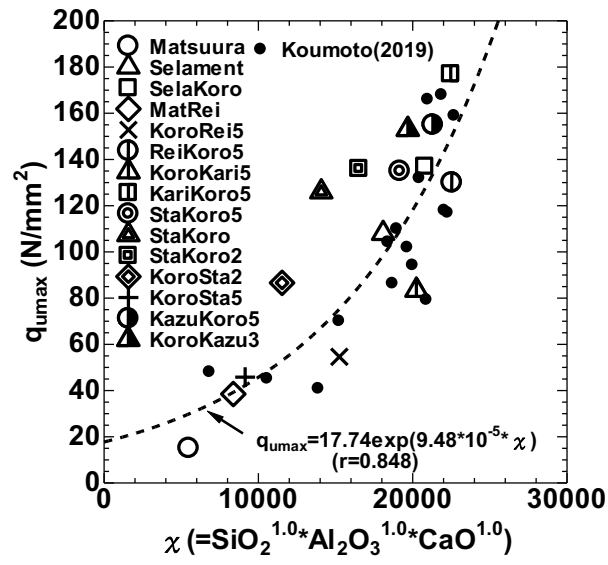
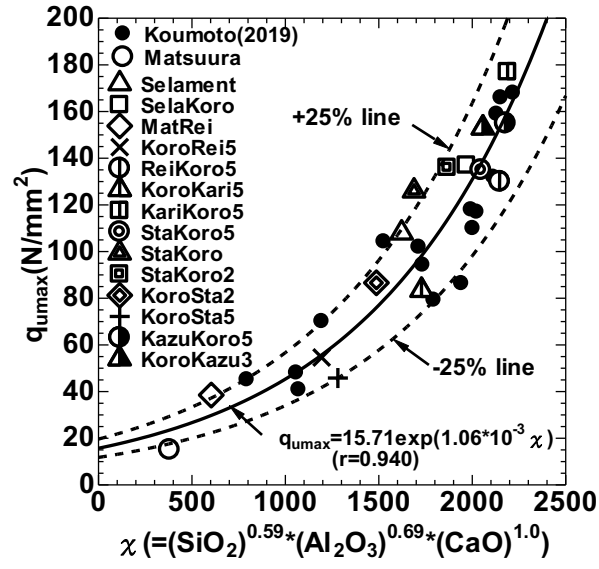


Fig. 10 Relationship between  $\Delta V/V$  and  $C_{cas}$



**Fig. 11 Relationship between  $q_{\max}$  and  $\chi$  ( $=\text{SiO}_2 \times \text{Al}_2\text{O}_3 \times \text{CaO}$ )**



**Fig. 12 Relationship between  $q_{umax}$  and  $\chi (= SiO_2^{0.59} \times Al_2O_3^{0.69} \times CaO^{1.0})$ .**